Electromagnetic Performance Analysis of Electrically Excited and Interior Permanent Magnet Motor for Electric Vehicle Application

Bui Minh Dinh
Hanoi University of Science and Technology (HUST)
dinh.buiminh@hust.edu.vn
Dinh Hai Linh
Vietnam Forestry University
Hailinh.vfu@gmail.com

Tieu Xuan Hoang, and Nguyen Huu Duc
Electric Power University
Hoangtx@epu.edu.vn, duc.nguyenhuu@epu.edu.vn

Abstract

This paper will compare and analyze an Electrically Excited Synchronous Motor (EESM) and Interior Permanent Magnet (IPM) machines for an electric vehicle application based on Volkwagen ID.3 2020. The Torque and Power performances of EESM can be improved in wide range of speed with the same machine size and power inverter in compared with the IPM machine. Efficiency maps of both machines are obtained and compared with iron losses calculated by finite element analyses. It shows that the EE machine can be a low-cost alternative to the IPM machine with slightly lower efficiency and maximum torque. Due to its adjustable excitation, the EE machine is able to achieve a wider constant power speed range than the IPM machine. However, the efficiency of the EE machine is not better than the IPM machine in the high-speed region, since flux weakening control via armature windings is still necessary.

This paper also presents a detailed design of three-phase interior permanent magnet (IPM) synchronous motors Electrically Excited Synchronous Motor (EESM) with minimum weight, and maximum power output for a wide constant-power range. The stator and rotor geometry of the two motors with several variables and constraints has been implemented to evaluate electromagnetic performances. The proposed motor design is based on both analytical models and special software to determine the magnetic sizes and geometry parameters of the stator and rotor. The experimental test and analytical results have been used to evaluate silicon steel material for designs.

Keywords:

Interior Permanent Magnet Motor-IPM Motor, Electrically Excited Synchronous Motor (EESM) Finite Element Analysis-FEA.

Introduction

The Electrically Excited synchronous motor (EESM) and interior permanent magnet motor (IPM) are proven by their nature to be promising options for use in an electric vehicle traction motor. This research focused on developing Electrically Excited synchronous motor (EESM) based on Interior Permanent Magnet Motor-IPM Motor Volkwagen ID.3 2020. The IPM motors built with magnets placed inside the rotor body are attracting great attention in several variable-speed applications, such as electric vehicles and industrial and domestic appliances, where the most challenging requirement are high efficiency, high torque density, good overload capability, and extended speed range. The performance of IPM machines is significantly affected by the magnet rotor topologies in Chen Peng 2021, Wenliang Zhao 2015. Thus, several Interior Permanent Magnet Synchronous Motor Design Trend are developing different topology rotor designs such as V-shaped from manufacturer Tesla; double V magnet shape from manufacturer China, delta shape from manufacturer AVL, hybrid delta shape based on the V shape from both manufacturer Tesla and manufacturer Nissan; hybrid double V shape from both manufacturer T and manufacturer V. Those design of rotor shape have aimed to maximize efficiency, torque density, overload load capability Chen Peng 2021, Wenliang Zhao 2015, Yang, Y 2017. However, this study will focus on comparing

power, torque and efficiency maps of EESM with IPM 150kW. This study will improve average torque current characteristic by hybrid rotor shape design and step skewing magnet segment. The orque and power vs current of the IPM step-skew magnet rotor are simulated to verify by FEA method.

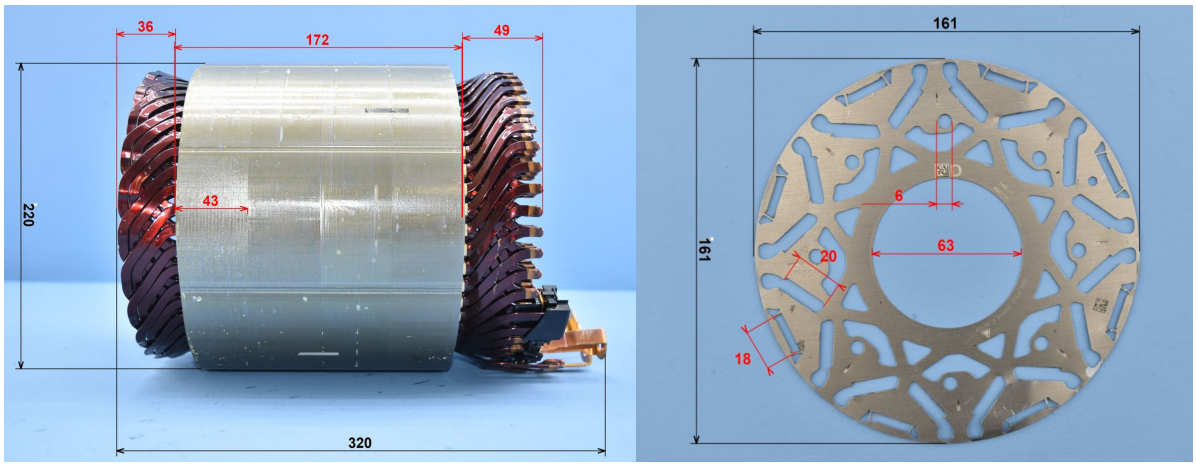

Figure 1. Stator Core and Rotor Lamination of IPM 150kW-16.000 rpm of on Volkwagen ID.3 2020

Table 1. Material requirement

Parameter	**Value**
Volkswagen ID.3	2020
Peak power kW	150
Winding Type	Hairpin
Stator assy weight	23.6
Stator LAM weight	17.98
Copper weight	5.388
kW/ Stator Assembly	6.36
kW/kg Copper	27.40
kW/ kg Stator Iron	8.30
Cooling system	Liquid cooling
Voltage	394

The main constraints are ratios of inner, outer stator/rotor, stator tooth and stator yoke and stack length. The Finite Element analysis is used to evaluate the motor performance and the design requirements (at base speed and maximum speed), namely, to compute the objective function values and constraints of the minimization problem which represents mathematically the optimal design problem, and which considers the parameters of the motor as independent variables. The optimization procedure uses the information obtained by the FE program to iteratively update the set of motor parameters and try to identify an “optimal” motor by making a trade-off between the different parameters of the machine.

Table 2. Geometry parameters

1	48 Slots, 8 Poles
2	Shaft diameter = 60mm
3	Rotor outer diameter = 161 mm
4	Stator inner diameter = 162.4 mm
5	Airgap length = 0.7 mm
6	Stator stack length = 140 mm

7	Rotor stack length = 141.6 mm
8	Average stack = 140.8 mm

2. Analytical Program of IPM and EESM Designs

The program was developed for the purpose of combining analytical calculations in MATLAB coupling to FEMM into one program. The analytical calculation has been used and stored in Matlab programming language; the program interface was developed by Matlab GUI. After calculating completion, a detailed rotor and stator lamination were exported to their drawings in dxf type. The analytical program is auto integrated 2D stator and rotor designs coupling to the simulation environment of FEMM. The output torque is taken by a block integral of the rotor blocks and the air gap flux density is obtained by integral function. All results will be stored in the database and used for further comparison. In addition, results that belonged to calculation progress and resulted in simulation progress are saved separately in 2 files. The program is divided into three main parts: analytical calculation, exporting drawing, and magnetic stimulation. There are also some supporting parts including the material library which also associate with the FEMM library.

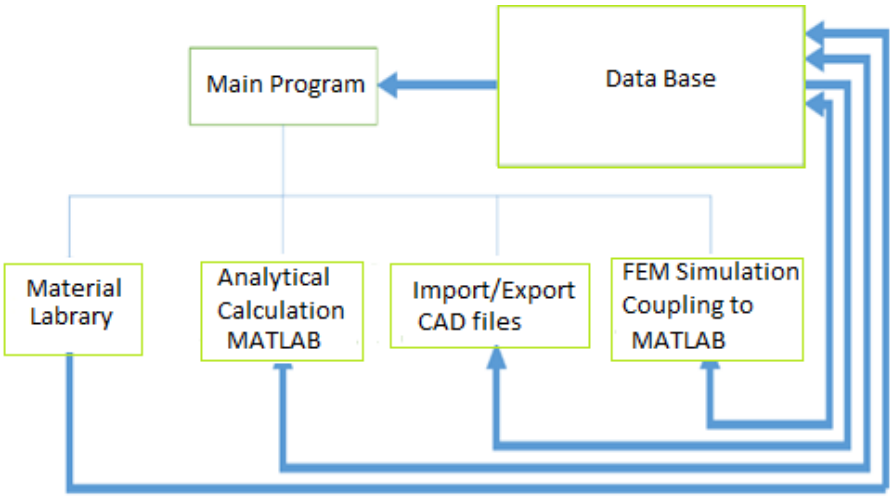

Figure 2. Analytical Program Structure

The proposal IPM and ÊM with 8 poles, 48 slots have PM in the delta arrangement. The main specifications of the original SynRM (without PMs) is shown in Table 1.

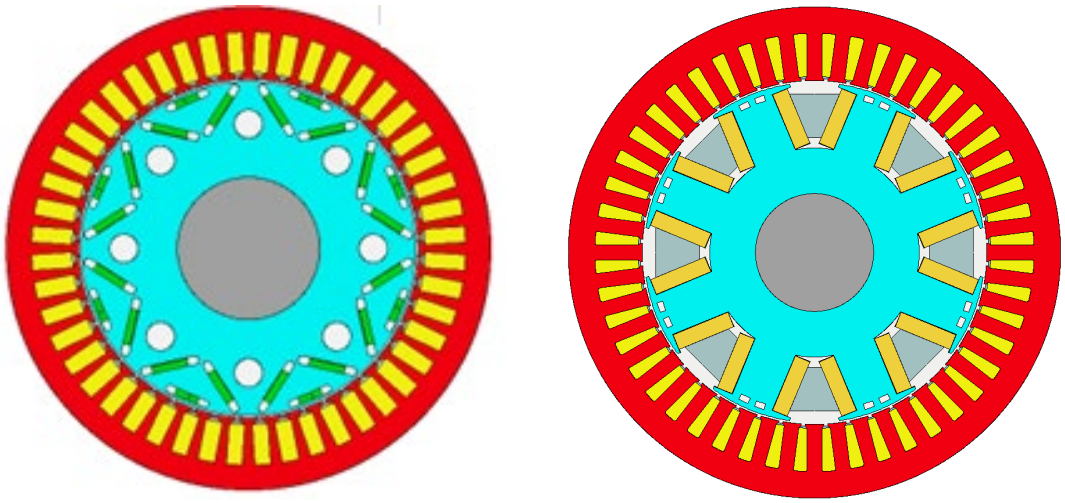

(a) (b)

Figure 3. Motor radial of IPM (a) and EESM Motors (b)

When a new electric machine is to be designed, the requirements usually include a set of performance specifications and a set of constraints or limitations such as the maximum physical size, the maximum temperature rise, and the supply voltage. This section explains how the basic size of a machine can be determined, starting from the performance specifications, and working within the limits of material properties and temperature rise. In many cases, new machine designs are evolved from existing ones, by modifying existing laminations and components to minimize the cost of changes in tooling and components. Even so, the same principles determine how much power and performance can be achieved from a machine of a given size and temperature rise. The flux and current densities are closely related to the power loss density which determines the cooling requirements and temperature distribution throughout the machine.

The number of slot and poles, stack length, the diameter of the stator and rotor, and the air-gap length listed in table 1 is designed for the power inverter of 396VDC/450 A, the continuous rated power of IPM is 80kW and peak power í 150kW, and the maximum speed of the machines is 20000 rpm. The geometry parameters of the stator and rotor can be calculated as follow the chart in figure 2. An analytical model was undergone many calculation steps to define basic parameters. Based on torque volume density TVR from 65 to 80 kNm/m3 [5], if we assume rotor diameter equal to rotor length, the rotor diameter D and length L sizes of IPM is determined as follow:

$$T = \frac{\pi}{4}.D^2.L_s.TRV \qquad (1)$$

With :

T : Electromagnetic torque (N.m).

D : Out diameter (m).

L_S : Length of core (m).

TVR : Torque and volume ratio (kNm/m3).

$$TRV = \frac{\pi}{\sqrt{2}} k_{W1} A.B \quad Nm/m^3 \qquad (2)$$

$$A = \frac{2m.N_{ph}I}{\pi\, D} \quad A/m \qquad (3)$$

The main parameters (such as outer diameter, rotor diameter, motor length, stator slot, and airgap length) are defined by considering some practical factors with desired input requirements. The main part of the process is to design the rotor configuration which is an embedded permanent magnet. The PM configuration needs to create sufficient magnetic voltage for the magnetic circuit. In fact, there are some possible configurations sorted by the shape and position of PM inside the rotor. Table 1 shows the design parameters of the two models such as the number of permanent magnet segments, pole, slot, and stack length. The material weight of IPM is summarized in table 2.

To calculate electromagnetic torque and power at synchronous speed, the phasor diagram is figured out in Fig 9. This is drawn for a salient-pole machine with X_d different from X_q. The voltage drops X_qI_q and X_dI_d, aligned along the d and q axes.

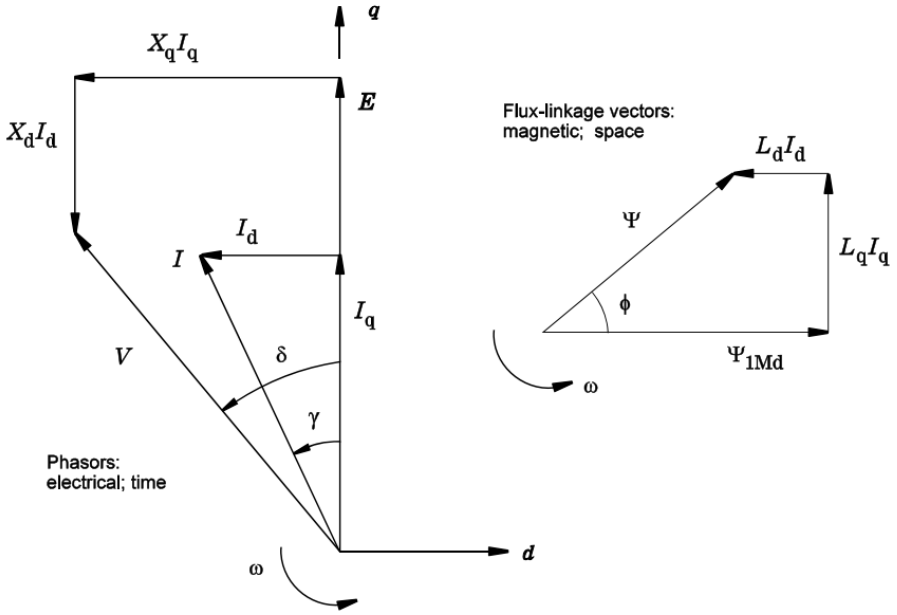

Figure 4. Phasor diagram of IPM and EESM

The voltage, and current phasor diagram is drawn for one phase of the IPM bad EESM, and it is assumed to be similar for the other phases such as phase B and phase C when three-phase balanced operation. The phasor diagram in Fig. 9 can be divided into two parts. On the left are the electrical quantities with voltages and currents. On the right are the corresponding magnetic flux linkages. The separation into two parts makes the diagram clearer. The flux-linkage part of the diagram is usually omitted, but it can be considered to have a physical reality, in that the flux rotates in space, at an angular velocity. The instantaneous physical orientation of the flux is also implicit in the related concept of space vectors. the phasors simply represent time-varying sinusoidal quantities.

$$I_d = -I \sin\gamma \text{ and } I_q = -I \cos\gamma \quad (4)$$

$$T = \frac{mp}{\omega}[EI_d + I_dI_q(X_d - X_q) \quad (5)$$

The flux-linkage produced by I_d is L_dI_d, where L_d is the *d*-axis synchronous inductance. It is in the phase with I_d and induces a voltage X_dI_d which is 90^0 ahead of *I*d (i.e., parallel to the *q* axis). $X_d = \omega L_d$ is the *d*-axis synchronous *reactance*. Like wise the current I_q produces a flux-linkage L_qI_q and a voltage $XqIq$ which is parallel to thenegad-axis axis, with $X_q = \omega L_q$ the *q*-axis synchronous reactance. The total the voltage at the phase terminals is the sum of the component voltages *E*, X_dI_d, and X_qI_q, added together "vectorially" by means of the polygon formed by the respective phasors placed nose-to-tail. Similarly, the total flux-linkage is the vector sum of the component flux-linkages ψ_{1M}, L_dI_d and L_qI_q.

In the PM machine, the wound poles are replaced by permanent magnets. but the meaning of the d and q axes is unchanged. An interior-magnet motor is a salient-pole machine with different inductive properties along the d- and q-axes apart from the magnetization of the magnets. The possibility of slight differences in permeability along the d- and q-axes. A further distinction can be made between "strong" and "weak" PM rotors ("PM-assisted reluctance motors"), but this is similar to the line-start permanent magnet motors

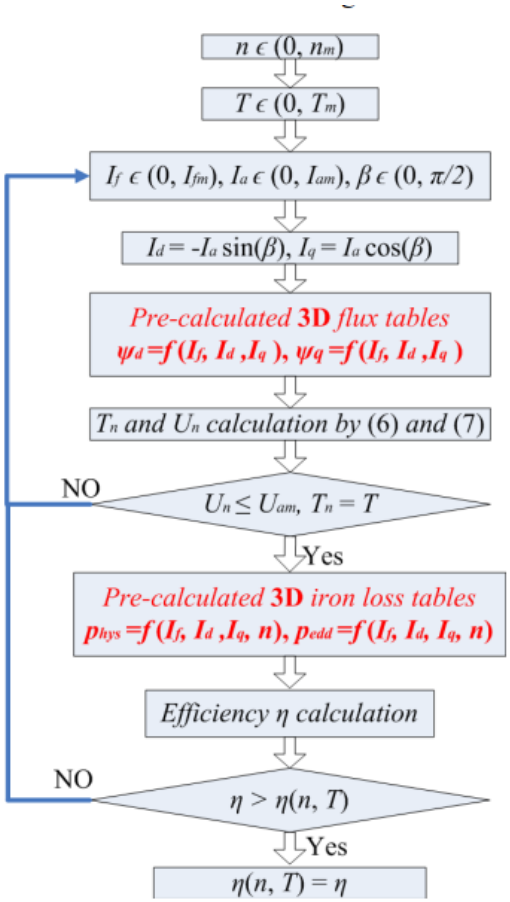

Figure 5. Analytical Calculation

3. Electromagnetic Performance Analysis

The design characteristics of the IPM and EESM are evaluated using finite element analysis (FEA). The flux density is given in Figure 6. As can be seen in 5b, the flux density of EESM is higher than that of the IPM. This is due to a higher excited current of EESM that is used in the EESM design. However, the total torque of the two motors is designed to be equivalent at the same current density by using full coil pitch windings on the double-layer IPMSM and short-pitch windings for the V-shaped one.

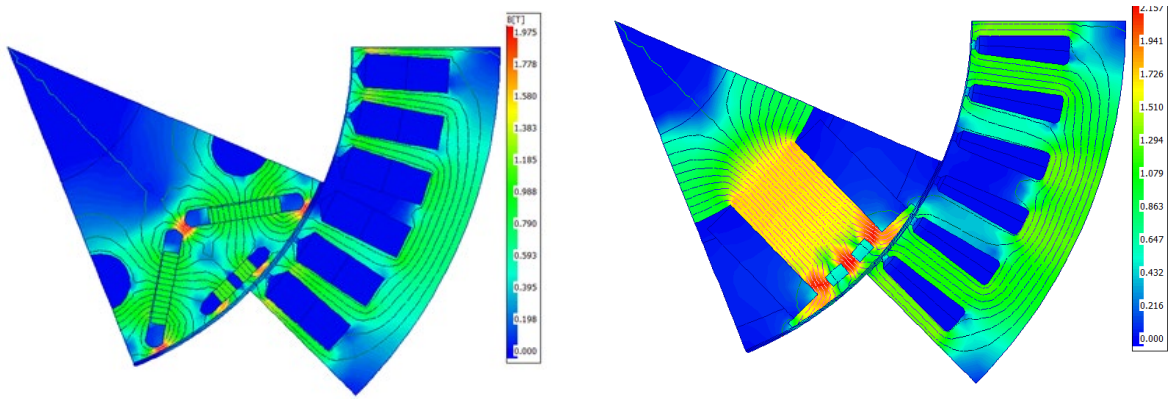

(a) (b)

Figure 6. Flux density distribution of IPM (a) and EESM Motors (b)

The Flux density waveforms of the conventional IPM and EESM motor are analyzed and compared by using no-linear finite element method (FEM) in Figure 7. It can be found that the proposed EESM motor has higher air-gap flux density, which benefits from the flux-concentration effect of excited coil configuration. It can be seen that the proposed motor offers a significantly higher no-load back-EMF than a conventional IPM motor.

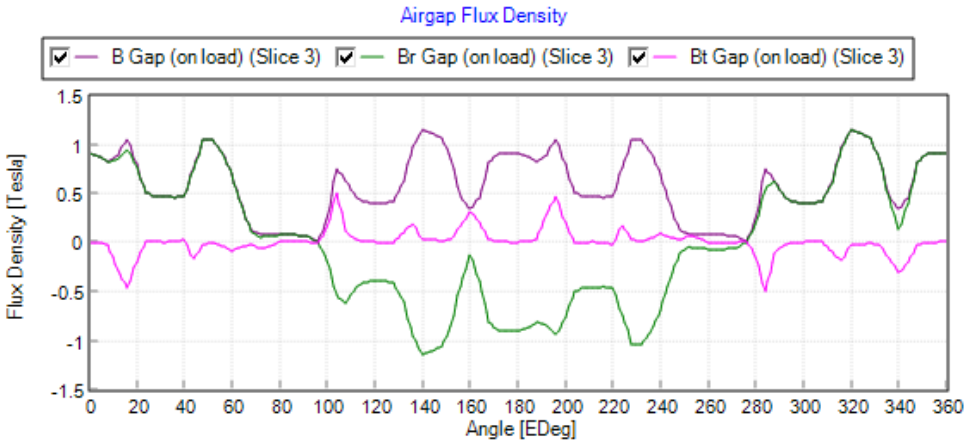

a. IPM

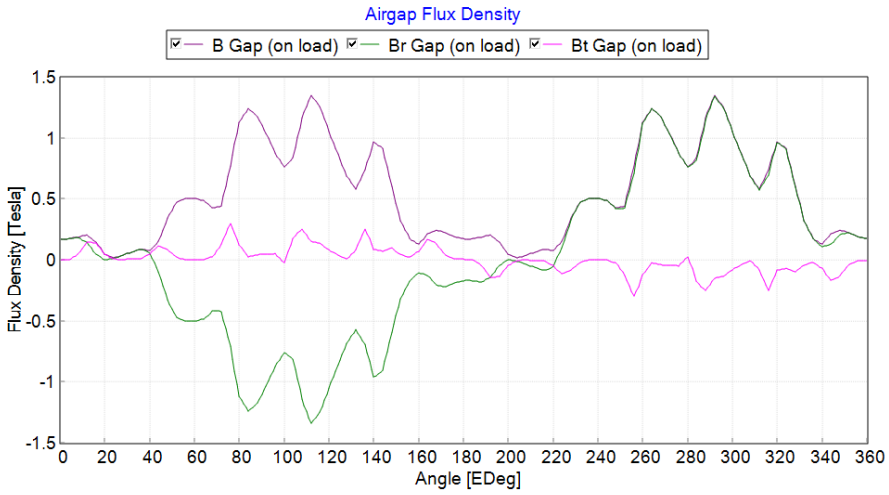

b. EESM

Figure 7. Flux density in the air gap

The torque waveforms of IPM and EESM are shown in figure 6. It shows that the IPM motor with step skewing rotor segment has higher average torque and lower ripples than the EESM. However, the average torque values is smaller.

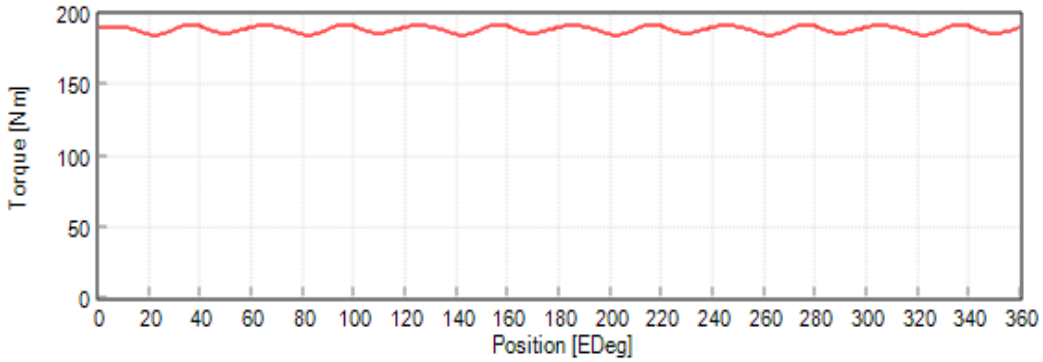

a. IPM

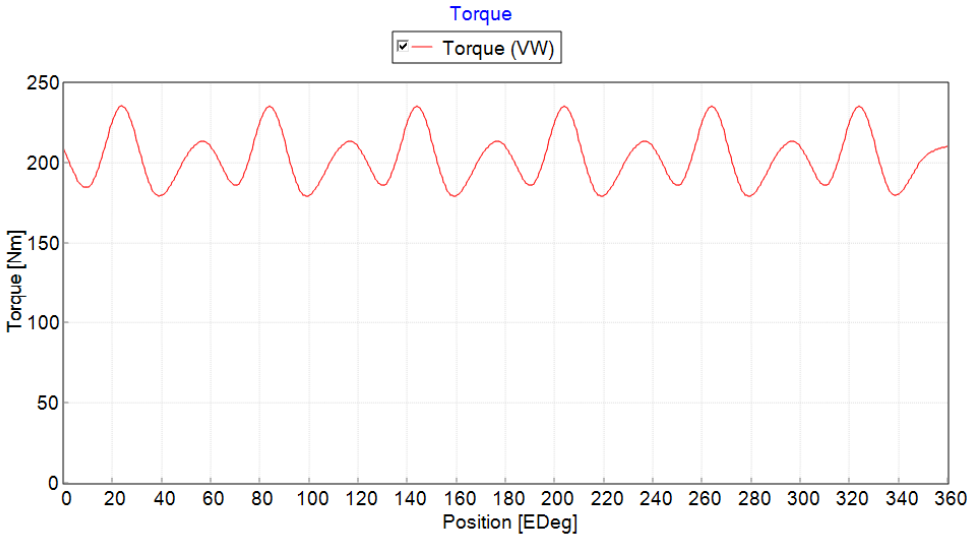

b. EESM

Figure 8. Average torque curve

Figure 9 shows the cogging torque versus the magnet span angle α of IPM and EESM. It is noted that with skewing the magnet span angle, the peak value of the cogging torque decreases with the increase of the step skewing rotor. It is interesting to find that the peak values of the cogging torque of EESM can also decrease with skewing stator or rotor. The cogging torque can be expressed by the integration of the normal and tangential magnetic flux components within the air gap. Because the normal and tangential magnetic flux components within the air gap vary with the geometry shape of pole shoes of the stator, the reduction of the cogging torque can be achieved by modifying pole shoes.

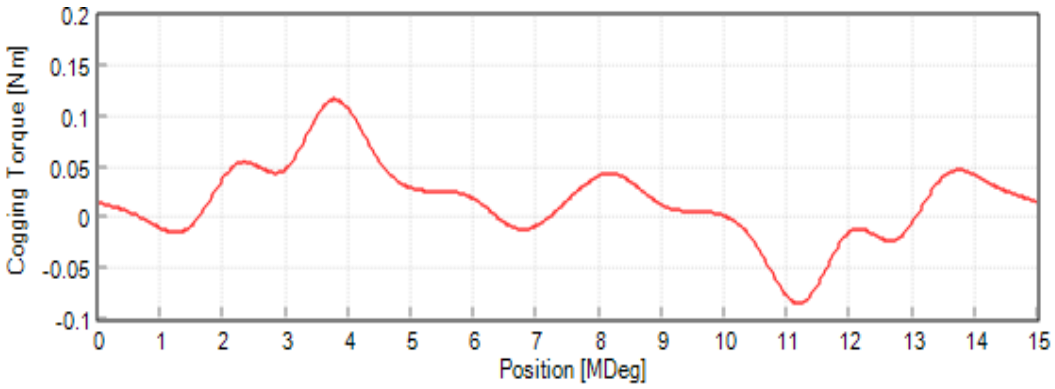

a. IPM

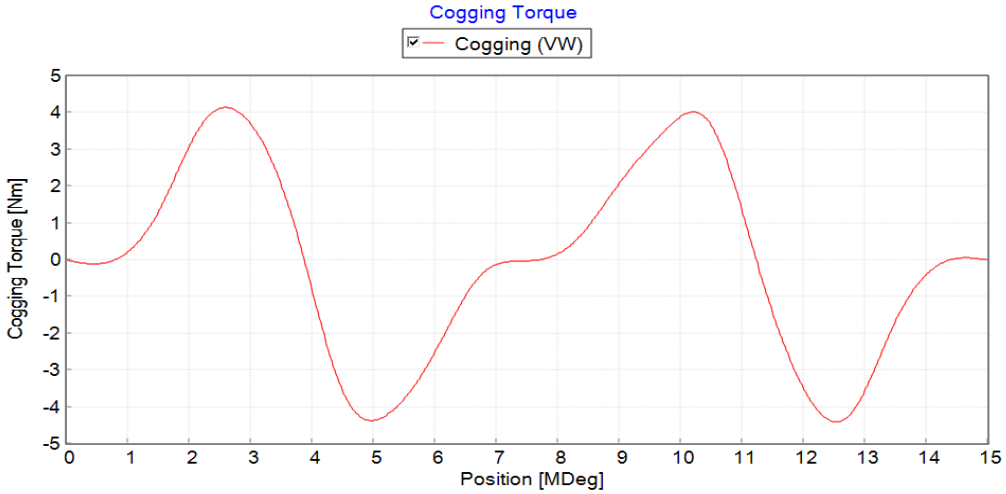

b. EESM

Figure 9. Cogging torque plot

The electromagnetic torque of an IPM machine is formed from two components of magnetic torque and reluctance torque. The PM component is produced based on the interaction between the air-gap magnetic field and armature reaction magnetic field and the reluctance component is instead on the asymmetry between the IPM machine's magnetic circuit of the d-axis and q-axis. The electromagnetic torque can then be defined as:

With the EE machine being optimized and its efficiency map calculated, the EE machine is comprehensively compared with the IPM machines at a base speed of 5000 rpm.

Table 3. IPM and EESM comparison

Parameters	**IPM**	**EESM**	**Unit**
Maximum torque possible	192.19	232.31	Nm
Average torque	167.49	233.46	Nm
Torque Ripple	3.3047	33.715	Nm
Torque Ripple [%]	1.9608	14.365	%
Cogging Torque Ripple (Vw)	0.63751	16.405	Nm
Speed limit for constant torque	6558.7	5152.4	rpm
No load speed	8661.5	4921.7	rpm
Electromagnetic Power	1.15E+05	98310	Watts
Input Power	1.16E+05	1.02E+05	Watts
Total Losses (on load)	2138.6	4652.4	Watts
Output Power	1.14E+05	97673	Watts
System Efficiency	98.158	95.453	%
Shaft Torque	167.42	233.18	Nm

The efficiency map of the IPM machine is obtained using the same principle and is shown in Fig. 8. The EE machine also has a lower efficiency than the IPM machine for the whole operation range. For further analyses, the detailed efficiency, loss, and power values at base operation points are compared in Table 3. It can be seen that for the same torque and speed, the iron losses of EE and IPM machines are very close. The lower efficiency of the EE machine results from the significantly higher copper loss. First, it is due to the excitation of copper loss. It should be noticed from Table 3 that even for EE machines flux weakening control is still required during high-speed operations. Lower d-axis flux linkage is achieved by the cancellation between excitation and negative *d*-axis currents but not by directly reducing the excitation current. Hence, the copper loss of the EE machine is not reduced but remains significantly high and the efficiency of the EE machine is still lower than the efficiency of the IPM machine in the high-speed regions. Second, the armature reaction is larger and hence the magnetic saturation is heavier in EE machines.

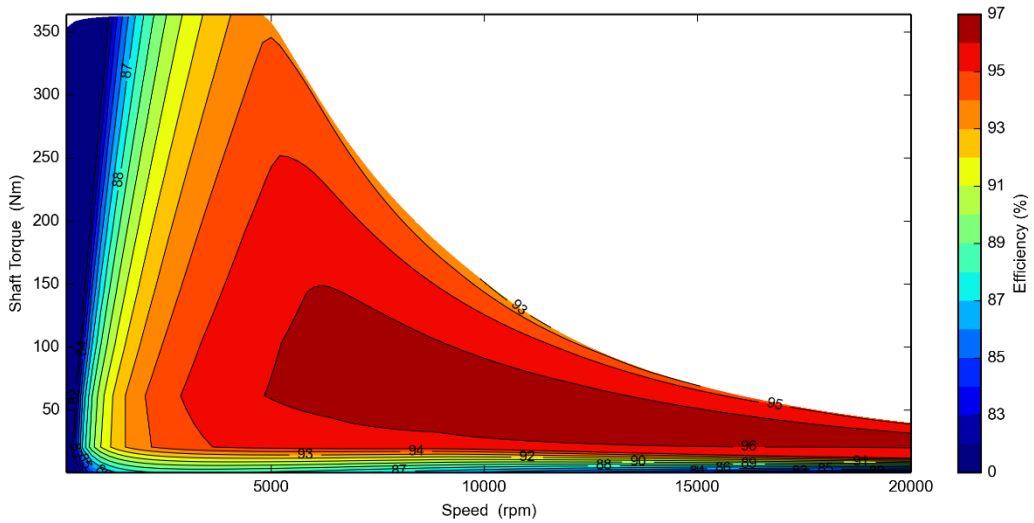

IPM efficiency map

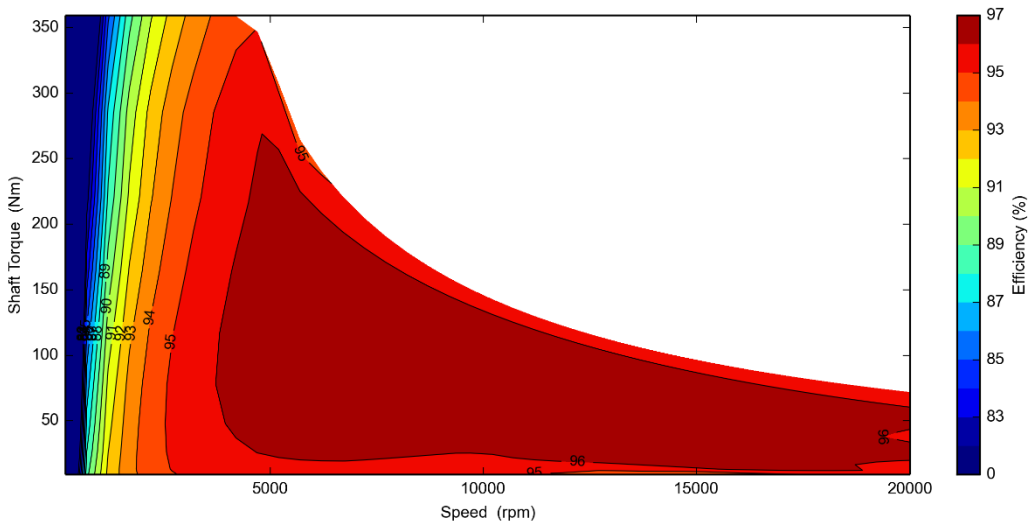

EESM efficiency map

Figure 10. IPM and EESM efficiency map comparison

Fig 8 shows that the maximum efficiency map of torque vs speed of the EESM is bigger than the IPM. With an efficiency of 96%, the maximum torque is 260Nm@5000rpm in EESM compared with 140N.m@5500 rpm. Especially, average torque values of EESM and IPM is 75N.m and 40 N.m at a maximum speed of 20.000 rpm

Conclusions

This paper has analyzed and compared torque, power and efficiency of a 3-phase 48-slot and 8-pole EESM and IPM motors for EV applications. The torque, power, and efficiency under peak torque performance and short overload have been measured at a maximum speed of 20000 rpm. A significant contribution of this study is to figure out EESM efficiency map improving in wide range speed in comparison with IPM motor 150kW for EV applications.

REFERENCES

Chen Peng;Daohan Wang;Zhenkang Feng;Bingdong Wang, *"A New Segmented Rotor to Mitigate Torque Ripple and Electromagnetic Vibration of Interior Permanent Magnet Machine"* IEEE Transactions on Industrial Electronics, Year: 2021 | Early Access Article | Publisher: IEEE

Wenliang Zhao;Thomas A. Lipo;Byung-Il Kwon*," Torque Pulsation Minimization in Spoke-type Interior Permanent Magnet Motors With Skewing and Sinusoidal Permanent Magnet Configurations"*, IEEE Transactions on Magnetics Year: 2015 | Volume: 51, Issue: 11 | Journal Article | Publisher: IEEE.

Wenliang Zhao;Thomas A. Lipo;Byung-Il Kwon, *"Torque Pulsation Minimization in Spoke-type Interior Permanent Magnet Motors With Skewing and Sinusoidal Permanent Magnet Configurations"* Year: 2015 | Volume: 51, Issue: 11 | Journal Article | Publisher: IEEE

Yildiriz, E.; Gulec, M.; Aydin, M. An Innovative Dual-Rotor Axial-Gap Flux-Switching Permanent-Magnet Machine Topology with Hybrid Excitation. *IEEE Trans. Magn.* **2018**

Li, W.; Ching, T.W.; Chau, K.T. Design and analysis of a new parallel-hybrid-excited linear vernier machine for oceanic wave power generation. *Appl. Energy* **2017**, *208*, 878–888, 2017.

Liu, Y.; Zhang, Z.; Zhang, X. Design and Optimization of Hybrid Excitation Synchronous Machines with Magnetic Shunting Rotor for Electric Vehicle Traction Applications. *IEEE Trans. Ind. Appl.* **2017**

Yang, Y.; Castano, S.; Yang, R.; Kasprzak, M.; Bilgin, B.; Sathyan, A.; Dadkhah, H.; Emadi, A. "*Design and Comparison of Interior Permanent Magnet Motor Topologies for Traction Application"*. IEEE Trans. Transp. Electrify. 2017, 3, 4–9, 2017.

Liu, X.; Lin, Q.; Fu, W. *"Optimal Design of Permanent Magnet Arrangement in Synchronous Motors".* Energies 2017, 10, 1700.

Wang, A.; Jia, Y.; Soong, W.L. "*Comparison of Five Topologies for an Interior Permanent-Magnet Machine for a Hybrid Electric Vehicle"*. IEEE Trans. Magn. 2011, 47, 3606–3609.

Bibliography:

Bui Minh Dinh is a Lecturer and researcher at Hanoi University of Science and Technology in Vietnam. He received a Ph.D. in Electric Motor Design and Manufacture in 2014 at the Technical University of Berlin, Germany, Among his research interests there are high-speed motor design and manufacture related to industrial products such as SRM, IPM, and IM motors. He has managed Viettel R&D for IDME design and Electromagnetic Advisor for Hanoi Electromechanical Manufacturer. Since 2019 he has been a technical advisor for several Electrical Vehicle Companies in Vietnam Such as M1 Viettel, Selex Motor Abaco, and Vinfast

Dinh Hai Linh is a Lecturer and researcher VFU in Vietnam. He received a Ph.D. in Electric Motor Design and Manufacture in 2022 at the Hanoi University of Science and Technology

Tieu Xuan Hoang is a Lecturer and researcher at EPU in Vietnam. He received a Master in EPU

Nguyen Huu Duc is a Lecturer and researcher at EPU in Vietnam. He received a Ph.D. in Electric Motor Design and Manufacture in 2014 at the Technical University of Berlin, Germany